24th COBEM - 2017

24th ABCM International Congress of Mechanical Engineering
December 3-8, 2017, Curitiba, PR, Brazil

COBEM-2017-0826
NUMERICAL SIMULATION OF NANOFLUIDS WORKING AS SECONDARY FLUID IN REFRIGERATION SYSTEM - A COMPARISON USING THERMOPHYSICAL PROPERTIES FROM MODELS AND MEASURED EXPERIMENTALLY

Felipe Lemos Renault
Abdul Orlando Cárdenas Gómez
Federal University of Uberlândia, Uberlândia, MG, Brazil
f.lemos.renault@gmail.com
orlandocardenas1589@gmail.com

Enio Pedone Bandarra Filho
Federal University of Uberlândia, Uberlândia, MG, Brazil
bandarra@ufu.br

Abstract. *This work is concerned with a comparison on measured and theoretical thermophysical properties of different nanofluids and use the properties to evaluate their suitability as a secondary working fluid in refrigeration systems, aiming at the external thermodynamic losses. Single-Walled Carbon Nanotubes (SWCNT) and silver nanoparticles were dispersed in distilled water to produce the nanofluid samples. A numerical simulation was performed taking into account a mathematical model for thermodynamic optimization of a heat exchanger. A comparison between the results obtained by the thermal properties measured experimentally and those ones evaluated theoretically by models were carried out, showing a notable difference among the results. The results evaluated with the experimental data show that in the case that the heat exchanger is optimized to minimize the external entropy generation, silver nanofluids (at any volumetric concentration) and the SWCNT nanofluids (at lower concentrations) presented positive results, whereas using the theoretical data indicated that silver nanofluids showed negative results and SWCNT nanofluids presented positive results both with any volumetric concentration.*

Keywords: *nanofluid, thermophysical properties, heat exchangers, external entropy generation.*

1. INTRODUCTION

One of the biggest challenges to increase the efficiency of different thermal systems is being able to enhance the heat transfer processes. On this note, academic and industrial groups had been directing their efforts in searching new materials, geometries or fluids that allow this intensification. One of the alternatives that arose with the advent of nanotecnology is to disperse particles with size between 1 - 100 nm in a usually base fluid to enhance its thermal properties, defined as nanofluid by Choi and Eastman (1995). Since the order of magnitude of the thermal conductivity of solid materials are at least 10 to 100 times bigger than those of conventional base fluids, dispersing nanoparticles of those materials in low fractions might intensify the thermophysical properties, while minimizing the problems associated with the mixture stability, as mentioned by Keblinski *et al.* (2002) and Chopkar *et al.* (2006).

Authors such as Prasher *et al.* (2006), Williams *et al.* (2008) and Timofeeva *et al.* (2009) agreed that nanofluids might present benefits on the thermal performance of a system, whenever there is an adequate balance between the increase of the thermal conductivity and the increase of viscosity. This way, the nanofluid's viscosity is also an important physical property, once other parameters such as pressure drop, pumping power and convective heat transfer are directly influenced by this property.

In this work, it was investigated the thermophysical properties of H_2O based suspension of silver nanoparticles and single-walled carbon nanotubes. After acquiring the thermophsyical properties of the nanofluids (through measurements and theoretical models), a simulation comparing the usage of the base fluid and the nanofluid as a secondary working fluid in a refrigeration system was run, based on the entropy generation minimization, as proposed by Pereira *et al.* (2015).

2. EXPERIMENTAL PROCEDURE

2.1 Synthesis of nanofluids

The method used for the production of nanofluids in this work is known as the two-step method. This method consists basically of the dispersion of nanoparticles, which are synthesized as a dry ultra-fine powder, in the base fluids by means of extra external energy which can be supplied by intensive magnetic stirring, ultrasonic agitation or homogenization at high pressure.

Two types of nanoparticles of different nature were used for the production of the nanofluids samples. The first type is metal based nanoparticles, specifically spherical silver (Ag) nanoparticles and the second type is carbon-based nanoparticles, specifically single-walled carbon nanotubes (SWCNT). The base fluid used was distilled water (H_2O). The nanoparticles used in the present work were provided by Nanostructures & Amorphous Material Inc., which also provided the thermophysical properties of nanoparticles.

Table 1 shows the nanofluids synthesized and used in the present work, naming the samples based on the volumetric concentration of nanoparticles dispersed on water.

Table 1: Volumetric concentration of the nanofluid samples

(Ag) Samples	**[% vol.]ϕ**	**(SWCNT) Samples**	**[% vol.]ϕ**
Ag_{01}	0.1	$SWCNT_{01}$	0.032
Ag_{02}	0.3	$SWCNT_{02}$	0.052
Ag_{03}	0.5	$SWCNT_{03}$	0.21

2.2 Density and Specific Heat of the Nanofluids

Assuming that the nanofluids are homogeneous fluids, once the nanoparticles are dispersed and stabilized within the base fluid, the density of the mixture can be calculated from the mixing rule used by Pak and Cho (1998), as shown in Eq. (1):

$$\rho_{nf} = (1-\phi)\rho_{bf} + \phi\rho_{np} \tag{1}$$

where ρ indicates the density and ϕ indicates the volumetric concentration of nanoparticles on the base fluid. The subscript nf indicates a property of the nanofluid, while bf is related to the base fluid and np to the nanoparticle.

The specific heat of the nanofluid samples was determined using a classical model based on the thermal equilibrium between the particles and the surrouding fluid. Applying the first law of thermodynamics, the mathematical model for calculating the specific heat of nanofluid is given by Eq. (2):

$$c_{p,nf} = \frac{(1-\phi)\rho_{bf}c_{p,bf} + \phi\rho_{np}c_{p,np}}{(1-\phi)\rho_{bf} + \phi\rho_{np}} \tag{2}$$

where c_p represents the specific heat of each component, followed by the appropriate subscripts. The density (ρ_{bf}) and specific heat ($c_{p,bf}$) of the base fluid were provided by the EES software database. The density (ρ_{np}) and specific heat ($c_{p,np}$) of the nanoparticle were supplied by the manufacturer as depicted in the Tab. 2.

Table 2: Geometric specifications and thermophysical properties of nanoparticles

Nanoparticle	**Geometric specifications**		**Thermophysical properties**	
	Length (l_{np})	**Diameter (d_{np})**	**Density (ρ)**	**Specific heat (c_p)**
Ag	[-]	20 nm	10.5 g/cm^3	0.23 kJ/(kg K)
SWCNT	5 - 30 μm	1 - 2 nm	2.1 g/cm^3	0.71 kJ/(kg K)

2.3 Measurement of thermal conductivity and dynamic viscosity

The thermal conductivity of SWNTC/H_2O and Ag/H_2O nanofluid samples was measured by the transient hot wire (THW) method. The Hukseflux TP-08 probe, also known as linear probe, was used. It is indicated for the evaluation of materials with thermal conductivity between 0.1 and 6 [W/m.K]. The measurement uncertainty of the equipment is $\pm$3% + 0.02 [W/m.K] as specified by the manufacturer. The process adopted for measurement is based on the guidelines of ASTM D5334-08, where the thermal conductivity is established as a function of the temperature-time relationship, the

geometric characteristics of the probe and the dissipated heat, with the hypothesis that the wire is an ideal heat source immersed in a homogeneous isotropic medium.

The viscosity measurements of the SWCNT/H_2O and Ag/H_2O nanofluid samples were made with a BrooKfield LDDV-IIIU, coneplate type rheometer with a measurement uncertainty $\pm 1\%$ of the full scale of the equipment, which is 3 [cP] plus 1% of the measured value). The shear stress of the sample is measured using an imposed deformation rate, in addition to determining the torque required to rotate the conical element. Due to the fact that apparently the viscosity of the samples are very close to the viscosity of the water, the rheometer was calibrated with distilled water at 25°C (μH_2O = 0.00089 [Pa.s]). The rotation of the equipment ranged from 110 to 180 rpm and the conical element used in the measurements was spindle CPE-41, requiring a 1 ml sample.

3. THERMOPHYSICAL PROPERTIES MEASURED EXPERIMENTALLY

3.1 Thermal Conductivity

Figure 1 shows the results of the thermal conductivity measurements of Ag/H_2O nanofluids as a function of the temperature, for different volume concentrations. The results presented an average increase of 8%, 19% and 37% of the thermal conductivity for the samples Ag_{01}, Ag_{02} and Ag_{03}, respectively for silver nanofluids over the base fluid. The values measured are compared to the thermal conductivity calculated through the model proposed by Gao and Zhou (2006), which are presented on Fig. 1 as the dashed lines, for each volumetric concentration.

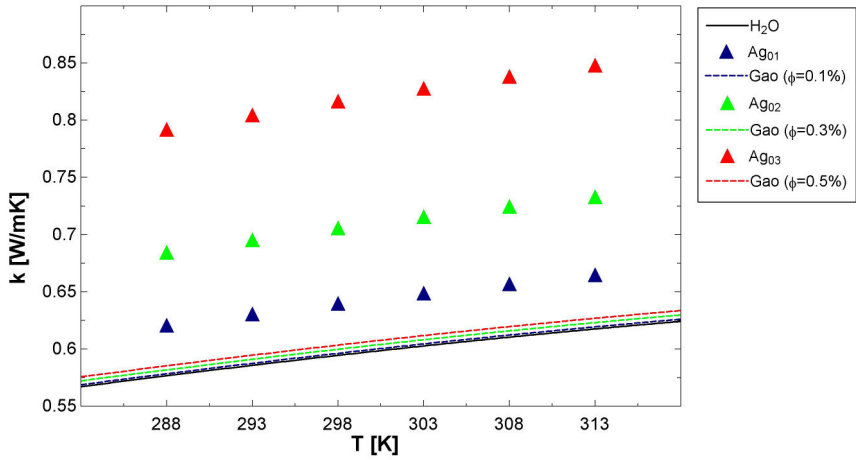

Figure 1: Thermal conductivity of Ag/H_2O nanofluids as a function of temperature

Figure 2 shows the results for SWCNT/H_2O nanofluids. The results showed an average increase of 11%, 24% and 29% of the thermal conductivity for the samples $SWCNT_{01}$, $SWCNT_{02}$ and $SWCNT_{03}$, respectively for SWCNT nanofluids over the base fluid. On the same figure, the dashed lines represent the thermal conductivity for each volumetric concentration calculated through the equation proposed by Xue (2006).

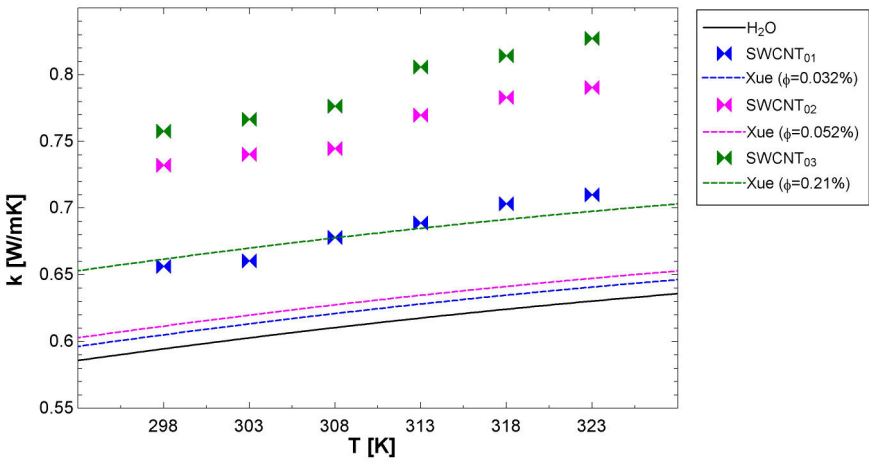

Figure 2: Thermal conductivity of SWCNT/H_2O nanofluids as a function of temperature

For both Silver and SWCNT nanofluids, it is important to highlight that the theoretical models underestimate the thermal conductivity in comparison with the experimental data, even when using small volume fractions of nanoparticles.

3.2 Dynamic viscosity

Five viscosity readings were acquired for each temperature analyzed. The result is the average of the five readings. As before, the values of the viscosity are presented as a function of the temperature. Figure 3 presents the results for the Ag/H_2O nanofluids. The sample Ag_{01} showed an average increase of 2% on its viscosity over the base fluid, while the sample Ag_{02} showed an average increase of 4% and the sample Ag_{03} showed an average increase of 6%. The measured results are compared to the theoretical values of the viscosity obtained by using the equation proposed by Maïga *et al.* (2004), presented on Fig. 3 for each volumetric concentration.

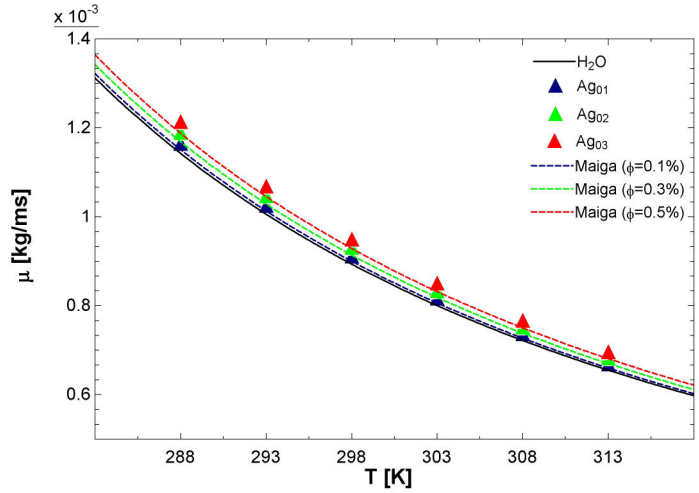

Figure 3: Dynamic viscosity of Ag/H_2O nanofluids as a function of temperature

Figure 4 shows the results for the SWCNT/H_2O nanofluids. The sample $SWCNT_{01}$ showed an average increase of 2% on its viscosity over the base fluid, while the sample $SWCNT_{02}$ showed an average increase of 11% and the sample $SWCNT_{03}$ showed an anomalous increase of 63%. The same model used previously to calculate the theoretical value of the viscosity is presented again on Fig. 4 for comparison between experimental and theoretical values.

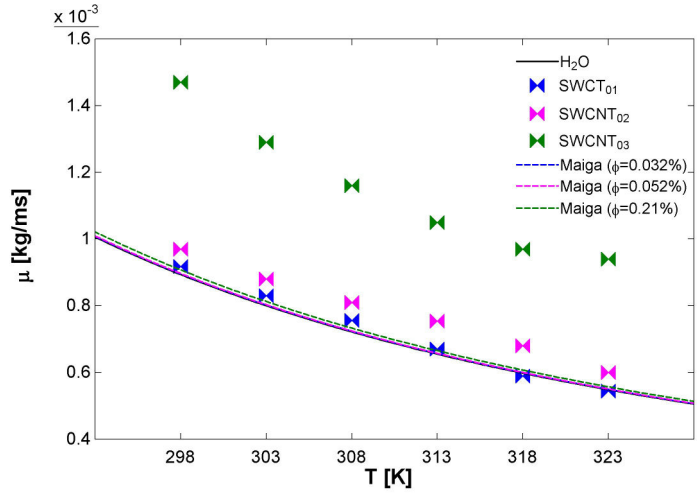

Figure 4: Dynamic viscosity of SWCNT/H_2O nanofluids as a function of temperature

The silver samples presented viscosity readings close to the expected values calculated through the theoretical model, whereas the SWCNT samples presented a much higher viscosity, even considering low volumetric concentrations ($\phi < 0.3\%$). One of the causes that can influence the high increase on this property is the amount of surfactant (NMP) used to produce the three samples, increasing the viscosity of the mixture even before adding the nanoparticles. Another reason for the high viscosity might be the geometric characteristics of the nanoparticles. Timofeeva *et al.* (2009) observed that nanofluids with nanoparticles of cylindrical or sheet formats presented higher viscosity than those with nanoparticles of sphere or spheroids, when using similar concentration in volume. This might be the cause for which the third sample

showed such a high increase on its viscosity, since the nanoparticle is a thin cylinder, with a relevant aspect ratio of $r = \frac{l}{d} = 11666$.

4. HEAT EXCHANGER SIMULATION

4.1 Physical Model

The next step after acquiring the thermophysical properties for each nanofluid is to simulate their use as a secondary working fluid in a condenser, which can be modelled as a double-pipe counter-flow heat exchanger with one stream changing phase, thus having an uniform temperature along the domain, having the secondary fluid's temperature changing from the inlet to the outlet (depending on the mass flow rate, heat transfer rate and the heat exchanger geometry). The modelled pipe is shown in Fig. 5 with a 10 mm bore and 10 m length, as proposed by Pereira *et al.* (2015).

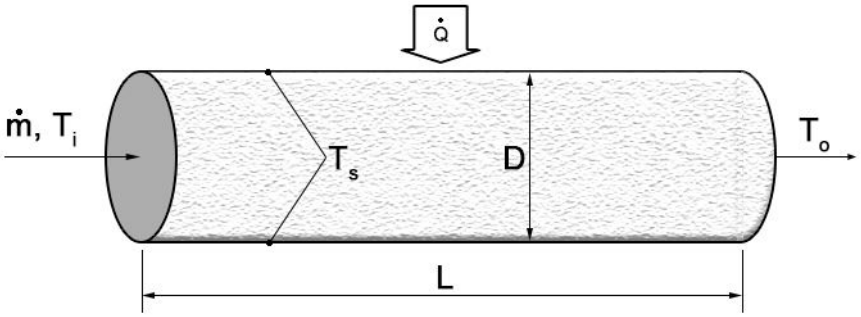

Figure 5: Physical model for the double-pipe heat exchanger

4.2 Mathematical Modelling

The complete details of the mathematical approach used in the present work can be found in Pereira *et al.* (2015) and the governing equations are following:

$$\dot{Q} = \dot{m}c_p(T_o - T_i) = \varepsilon\dot{m}c_p(T_s - T_i) \tag{3}$$

$$\varepsilon = 1 - exp(-NTU) \tag{4}$$

$$NTU = St\frac{A_s}{A_c} \tag{5}$$

$$St = \frac{Nu}{RePr} \tag{6}$$

$$\Delta p = p_i - p_o = \frac{1}{8}f\rho u_c^2\frac{A_s}{A_c} \tag{7}$$

$$T_{avg}(s_o - s_i) = c_p(T_o - T_i) + \frac{(p_i - p_o)}{\rho} \tag{8}$$

$$\dot{m}(s_o - s_i) = \frac{Q}{T_s} + \dot{S}_g \tag{9}$$

$$N_s = \frac{\dot{S}_g}{\dot{m}c_p} = \frac{\dot{Q}}{\dot{m}c_p}\left(\frac{T_s - T_{avg}}{T_s T_{avg}}\right) + \frac{fu_c^2}{8c_p T_{avg}}\frac{A_s}{A_c} \tag{10}$$

$$\frac{A_s}{A_c} = \frac{NTUPr^{2/3}}{j} \tag{11}$$

$$N_s = \frac{\Theta^2}{NTU} + \frac{f}{8j} EcPr^{2/3}NTU \tag{12}$$

$$Ec = \frac{u_c^2}{c_p T_{avg}} \tag{13}$$

$$\Theta = \frac{(T_o - T_i)}{T_s} \tag{14}$$

$$\frac{\partial N_s}{\partial NTU} = 0 \Rightarrow NTU^* = \frac{\Theta}{Ec^{1/2}Pr^{1/3}}\sqrt{\frac{8j}{f}} \tag{15}$$

The density and specific heat of the nanofluid can be obtained as shown by Eqs. (1) and (2), as described in the Section 2.

4.3 Discussion

The first analysis was carried out by constraining the heat exchanger geometry as proposed earlier ($D = 10\ mm$ and $L = 10\ m$) and its working conditions similar to those proposed by Pereira *et al.* (2015), fixing a heat duty of $\dot{Q} = 5.0\ kW$ and an average secondary working fluid temperature of $T_{avg} = 0.5(T_i + T_o) = 298\ K$, to make sure the nanofluids' properties used match the available measured temperatures. The positive heat transfer rate means that the secondary fluid is receiving heat from the refrigerant, which is the typical behavior of condensers.

Figure 6 shows the dimensionless entropy generation as a function of the number of transfer units for the Ag/H_2O nanofluid with different volume concentrations. The solid lines represent the results using the measured properties, while the dashed lines are the results obtained using theoretical models for the properties. It is possible to highlight that, for the experimental properties, with an increase of the volumetric concentration of nanoparticles in the nanofluid, there is virtually no increase to the minimum entropy generation rate possible, while there is a significant gain to the NTU of the heat exchanger for that point (minimum N_s). The theoretical models greatly underestimate the NTU increment, maintaining a behavior closer to the base fluid.

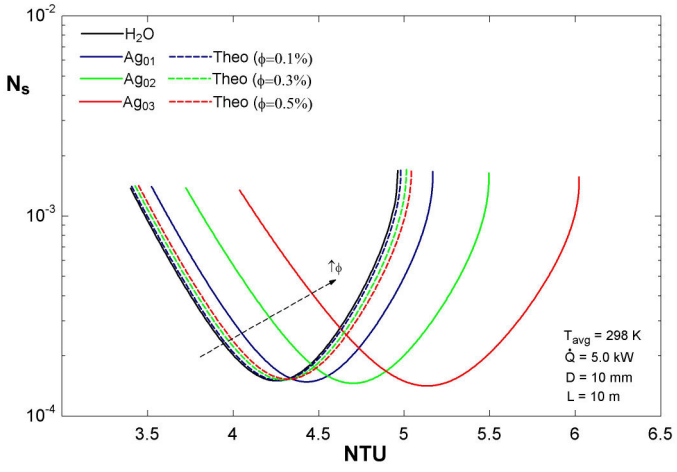

Figure 6: Variation of the entropy generation number with the number of transfer units for Ag/H_2O nanofluids

Figure 7 shows the ratio between NTU and the optimal calculated from Eq. (15) (NTU^*), where a ratio equals to one represents the minimum entropy generation rate observed on Fig. 6. It is worth noting that the flow conditions (expressed by Re) on the minimum entropy generation point differs with the addition of nanoparticles, due to the increasing viscosity.

The results obtained using theoretical properties were very close to the base fluid itself, and they were omitted to avoid clumping the figure.

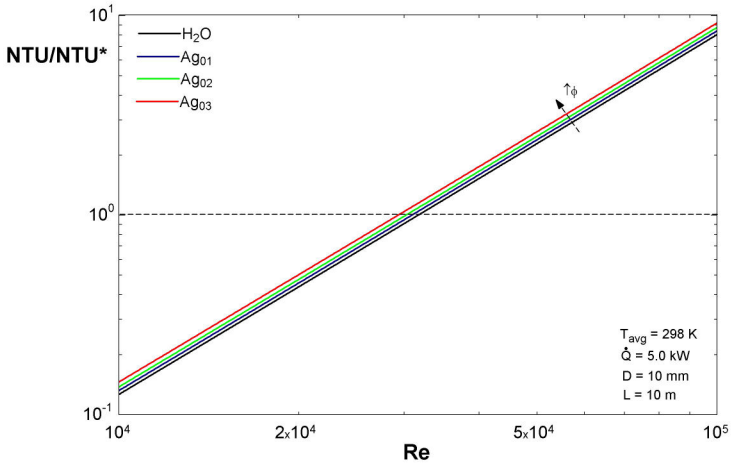

Figure 7: Variation of the $NTU \ / \ NTU^*$ with Reynolds for Ag/H_2O nanofluids

Figure 8 shows the results basically using the same conditions, just changing the nanofluid, SWCNT/H_2O. For the samples $SWCNT_{01}$ and $SWCNT_{02}$ (lower concentrations), the NUT value on the minimum entropy generation point increased, while the sample $SWCNT_{03}$ not only presented a lower NUT on that point, however also a slightly increase on the value of the minimum N_s. This can be explained by analyzing the properties presented on Section 3. For this sample, the increase of its thermal conductivity is similar to the sample $SWCNT_{02}$, which has a much lower concentration of nanoparticles, while it shows a significant increase on its viscosity (an average of 63.39% increase over the base fluid, compared to 11.49% increase for the sample $SWCNT_{02}$).

The results obtained using theoretical properties did not present this abnormal behavior, since it cannot predict the high increase on the viscosity for the third sample.

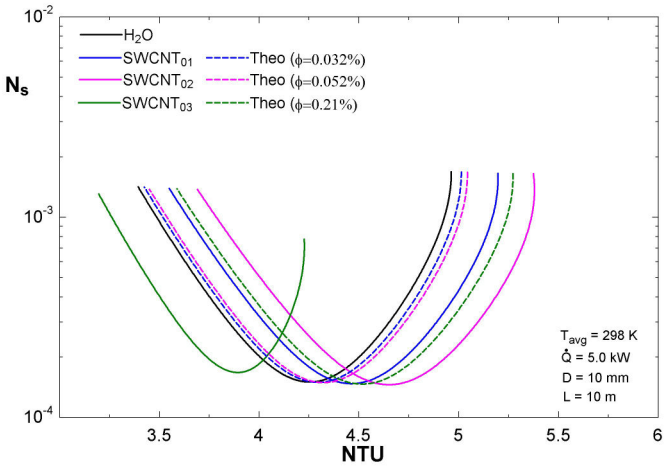

Figure 8: Variation of the entropy generation number with the number of transfer units for SWCNT/H_2O nanofluids

The effect of the higher viscosity of the sample $SWCNT_{03}$ is also seen in Fig. 9, where the high value of the viscosity strongly affect the Re value for this sample. The results using theoretical properties were very close to the base fluid for lower volumetric concentrations. Therefore, only the result for the higher volumetric concentration was presented on this figure.

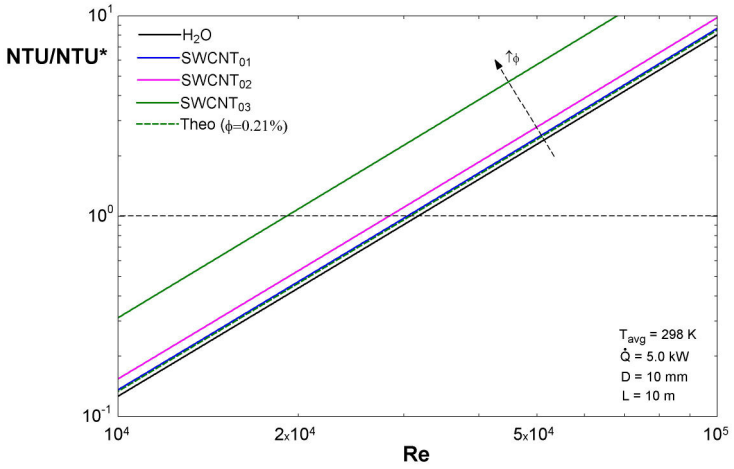

Figure 9: Variation of the $NTU \ / \ NTU^*$ with Reynolds for SWCNT/H_2O nanofluids

The second analysis consist in constricting the minimum entropy generation rate condition ($NTU = NTU^*$) - an analysis also proposed by Pereira *et al.* (2015), leaving the coil temperature free to vary. Figure 10 shows the pumping power for different heat transfer rates and volumetric fractions of silver nanoparticles dispersed in water, using a typical condition found in condensers ($\dot{Q} > 0$). For a fixed heat duty, less pumping power is required for higher volume fractions of nanoparticles, when considering the measured properties. However, when using the models to obtain the properties, the low volumetric concentrations imply in virtually no change in the results. A higher volume fraction ($\phi = 2.5\%$) was added to allow understanding of the behavior expected by the theoretical models, showing that the theoretical models predict an increase of the required pumping power for a fixed heat duty.

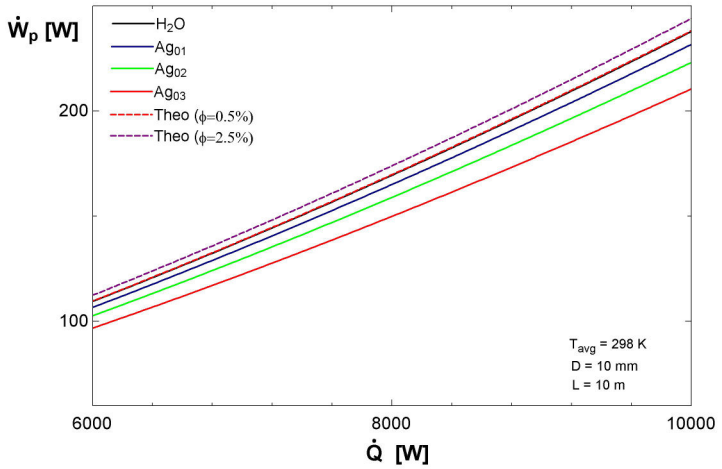

Figure 10: Variation of the pumping power with heat duty for Ag/H_2O nanofluids

The same behavior is observed analyzing the variation of the local rate of entropy generation with the variation of the heat duty. For a fixed heat duty, the local rate of entropy generation decreased with the increase of the volume fraction of nanoparticles, as seen in Fig 11, whereas the models predict the opposite.

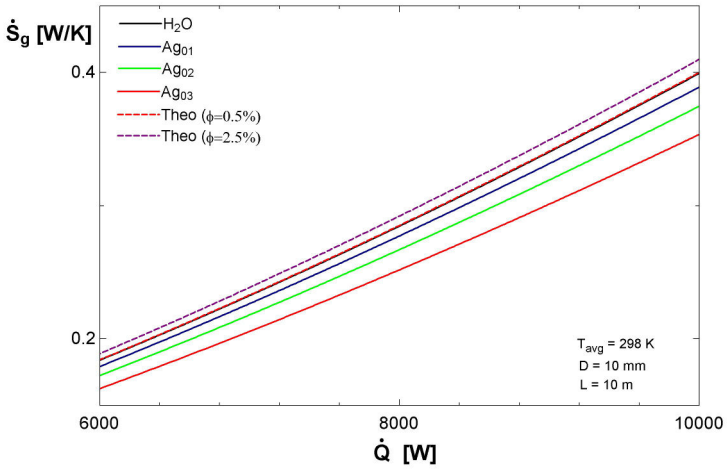

Figure 11: Variation of the local rate of entropy generation with heat duty for Ag/H_2O nanofluids

Figure 12 presents the same analysis however using the SWCNT nanofluids. As expected, the sample $SWCNT_{03}$ shows that the pumping power required for a fixed heat duty is bigger when compared to the base fluid, once its NUT for the minimal entropy generation condition was lower than the base fluid. The samples $SWCNT_{01}$ and $SWCNT_{02}$, with lower volumetric concentrations of nanoparticles, presented a positive result considering the use of the nanofluid over the base fluid.

For the lower concentrations, the models also predict a positive result, however with higher pumping power for a fixed heat duty when compared to the results obtained using measured properties. For the higher volumetric concentration ($\phi = 0.21\%$), however, the model still present a positive result, while the result of the sample $SWCNT_{03}$ showed a negative result, due to the high viscosity increase in the sample not predicted by the model.

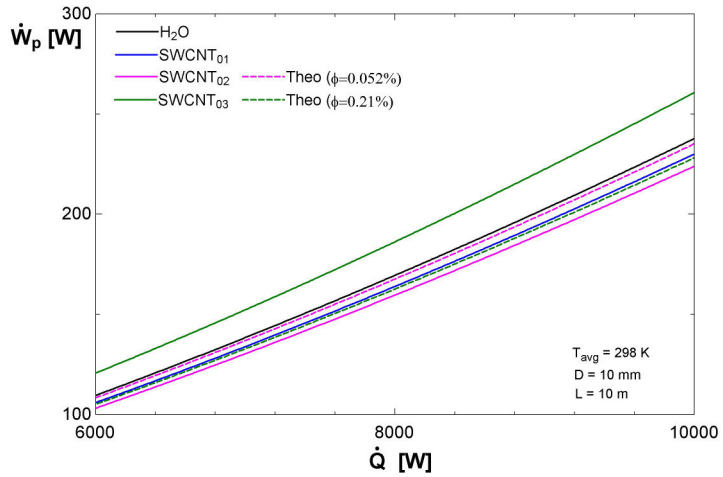

Figure 12: Variation of the pumping power with heat duty for SWCNT/H_2O nanofluids

The local entropy generation as a function of the heat duty for the SWCNT nanofluids are presented in Fig. 13. The nanofluids with lower concentration produce less entropy, while the nanofluid with the highest concentration produces more entropy, when compared to the base fluid.

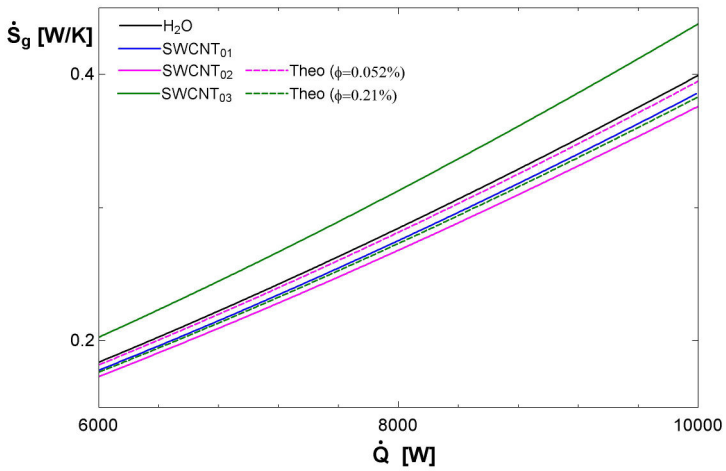

Figure 13: Variation of the local rate of entropy generation with heat duty for SWCNT/H_2O nanofluids

5. CONCLUSIONS

The thermophysical properties of H_2O based Silver and Single-Walled Carbon Nanotubes (SWCNT) nanofluids were experimentally measured and calculated through theoretical models, and used as parameters for an investigation of their suitability as secondary working fluids in a condenser, aiming at the external thermodynamical losses, by means of an Entropy Generation Minimization analysis. This investigation was carried out using numerical simulations considering a double-pipe heat exchanger as used in Pereira *et al.* (2015). It is interesting to note that the same analysis conducted for the condenser can also be conducted for the evaporator, by simply applying a negative value to the heat duty ($\dot{Q} < 0$).

As observed by Pereira *et al.* (2015), it is verified the existence of a NTU which minimizes the dimensionless entropy generation rate (N_s). For the conditions tested, the silver nanofluids presented a higher NUT with which the dimensionless entropy generation rate is minimized, while maintaining the minimum N_s roughly at the same value, when compared to water. The SWCNT nanofluids presented similar results for lower volumetric concentrations of nanoparticles (0.032% and 0.052%), while a higher concentration of nanoparticles (0.21%) caused a large increase in the viscosity.

For the experimental data collected, it was observed that the silver nanofluids require less pumping power and generate less entropy to accomplish the same heat duty, when compared to water. This trend is observed for the samples $SWCNT_{01}$ and $SWCNT_{02}$, while only the sample with higher concentration of nanoparticles, $SWCNT_{03}$, presented a higher pumping power required for a fixed heat duty, when compared to water, also generating more entropy.

For the data obtained through theoretical models, the addition of silver nanoparticles to the base fluid would only cause a notable difference for higher volumetric concentrations than those used in the samples. Also, the models predicted a higher required pumping power and entropy generation for a fixed heat duty when using silver nanofluids instead of the base fluid. For the SWCNT nanofluids, the model predicted similar results than the first two samples, however predicted that the higher volumetric concentration ($\phi = 0.21\%$) would be effective, whereas the result for the third sample indicated the opposite.

This shows that the theoretical models to estimate the thermophysical properties of nanofluids must be used with caution, since they might underestimate the thermal conductivity in some cases, and might not be able to predict some changes in properties, such as the viscosity increase due to geometric characteristics of the nanoparticles.

The results indicates that some nanofluids might present good perspectives to be used as secondary working fluids in refrigeration systems, requiring a proper analysis and measurements of its thermophysical properties to evaluate the effects caused by those properties, when comparing to the base fluid. Also, this work is aimed solely on the external thermodynamical losses, requiring an analysis over the internal losses that takes place on a condenser or evaporator before stating the suitability of the nanofluids.

6. ACKNOWLEDGEMENTS

The authors gratefully acknowledge the support given to this investigation by CAPES, CNPq and Fapemig. The authors would also like to extend their recognition to Prof. Christian Hermes from POLO-UFSC for his valuable comments and provided the program used in this work.

7. REFERENCES

Bejan, A., 1987. "The thermodynamic design of heat and mass transfer processes and devices". In *International Journal of Heat and Fluid Flow, vol.8, Issue 4*. Durham, NC, USA.

Choi, S.U.S. and Eastman, J.A., 1995. "Enhancing thermal conductivity of fluids with nanoparticles". In *International Mechanical Engineering Congress and Exposition*. Argonne, IL, USA.

Chopkar, M., Das, P.K. and Mannaa, I., 2006. "Synthesis and characterization of nanofluid for advanced heat transfer applications". In *Scripta Materialia, vol. 55, Issue 6*. Kharagpur, India.

Gao, L. and Zhou, X.F., 2006. "Differential effective medium theory for thermal conductivity in nanofluids". In *Physics Letters A, vol.348, Issues 3-6*. Suzhou, China.

Incropera, F.P., Dewitt, D.P., Bergman, T.L. and Lavine, A.S., 2006. *Fundamentals of Heat and Mass Transfer*. John Wiley & Sons, South Bend, IN, USA, 6th edition.

Kays, W.M. and London, A.L., 1984. *Compact Heat Exchangers*. McGraw-Hill, Sydney, Australia, 3rd edition.

Keblinski, P., Phillpot, S.R., Choi, S.U.S. and Eastman, J.A., 2002. "Mechanisms of heat flow in suspensions of nano-sized particles (nanofluids)". In *International Journal of Heat and Mass Transfer, vol. 45, Issue 4*. Troy, NY, USA.

Maïga, S.E.B., Nguyen, C.T., Galanis, N. and Roy, G., 2004. "Heat transfer behaviours of nanofluids in a uniformly heated tube". In *Superlattices and Microstructures, vol.35, Issues 3-6*. Moncton, Canada.

Pak, B.C. and Cho, Y.I., 1998. "Hydrodynamic and heat transfer study of dispersed fluids with submicron metallic oxide particles". In *Experimental Heat Transfer, vol.11, Issue 2*. Jeonju, Korea.

Pereira, R., Loyola, F.R., Jr, W.L.S., Cardoso, R.P. and Hermes, C.J.L., 2015. "Thermodynamic assessment of water-alumina nanofluids as secondary working fluids in refrigeration systems aiming at the external irreversibilities of the cycle". In *International Congress of Refrigeration, Yokohama, Japan*. Curitiba, Brazil.

Prasher, R., Song, D. and Wang, J., 2006. "Measurements of nanofluid viscosity and its implications for thermal applications". In *Applied Physics Letters, vol. 89, Issue 23*. Chandler, AZ, USA.

Timofeeva, E.V., Routbort, J.L. and Singh, D., 2009. "Particle shape effects on thermophysical properties of alumina nanofluids". In *Jornal of Applied Physics, vol. 106, Issue 1*. Argonne, IL, USA.

Williams, W., Buongiorno, J. and Hu, L.W., 2008. "Experimental Investigation of Turbulent Convective Heat Transfer and Pressure Loss of Alumina/Water and Zirconia/Water Nanoparticle Colloids (Nanofluids) in Horizontal Tubes". In *Jornal of Heat Transfer, vol. 130, Issue 4*. Cambridge, MA, USA.

Xue, Q.Z., 2006. "Model for the effective thermal conductivity of carbon nanotube composites". In *Nanotechnology, vol.7, Number 6*. Beijing, China.

8. RESPONSIBILITY NOTICE

The authors are the only responsible for the printed material included in this paper.